LIDAR measurements of cirrus clouds in the northern and southern midlatitudes during INCA (55°N, 53°S): A comparative study

Franz Immler and Otto Schrems

Alfred Wegener Institute for Polar and Marine Research, Bremerhaven, Germany

Received 8 March 2002; accepted 5 June 2002; published 29 August 2002.

[1] Cirrus clouds have been probed at two locations in the midlatitudes of the southern (SH) and northern hemisphere (NH) with a Mobile Raman Aerosol Lidar (MARL) as part of the European INCA field experiments in 2000. MARL offers the opportunity to observe visible and subvisible clouds and to determine the optical depth τ in a range from below 10^{-3} up to 3. Despite different synoptic conditions we find at both locations similar macrophysical cloud properties, like mean base and top temperature among others. The frequencies of the optical depth show a characteristic distribution with a high share of subvisible clouds at both locations. While thin haze layers are frequently detected in the NH alone, we find highly depolarizing cirrus clouds only in the SH. These differences indicate that different cirrus properties and formation mechanisms are present at the two sites. *INDEX TERMS:* 0320 Atmospheric Composition and Structure: Cloud physics and chemistry; 0305 Atmospheric Composition and Structure: Aerosols and particles (0345, 4801); 0394 Atmospheric Composition and Structure: Instruments and techniques.

1. Introduction

[2] The important impact of cirrus clouds on the earth radiation budget and thus on climate has often been adressed [*Liou*, 1986], however the processes of cloud formation and its radiative behavior are not yet well understood. Subvisible cirrus (SVC), defined as an ice cloud with an optical depth τ below 0.03 [*Sassen et al.*, 1989], has recently been reported to be abundant not only in the tropics, but also in the midlatitudes. Satellite data suggest a slightly higher occurrence frequency in the northern hemisphere compared to the southern hemisphere [*Wang et al.*, 1996]. SVCs can have a direct effect on climate but more importantly may play a crucial role in the formation process of visible cirrus clouds, since there are indications that the cirrus formation goes through a haze state before reaching its final crystal size and habit [*Heintzenberg et al.*, 1995]. The cirrus radiative forcing is extremely sensitive to the properties and size distribution of the particles [*Zhang et al.*, 1999].

[3] The lidar method offers the opportunity to detect cirrus over a wide range of optical depths. The objective of our work was to supply two comparable datasets on midlatitude cirrus from the southern and the northern hemisphere with the same instrument and to analyze it in respect to differences that may result from fundamentally different aerosol loadings. These are caused by larger northern hemispheric source regions for continental aerosols (mineral dust) and by anthropogenic emissions [*Tegen et al.*, 1997].

[4] As part of the European INCA 2000 project (Interhemispheric differences in cirrus cloud properties by anthropogenic emissions), we probed cirrus clouds under comparable conditions, as far as latitude and season is concerned, with a mobile Raman Lidar. INCA laid a basis for a joint effort of institutes from the German Helmholtz Association to determine the effect of particles emitted by aircraft on contrails, cirrus clouds and climate (PAZI). The campaigns took place during March/April 2000 in Punta Arenas/Chile (53.12°S, 70.88°W; hereafter PA) and during September/October 2000 in Prestwick/Scotland (55.51°N, 4.60°W; hereafter PW). Recently, climatologies of cirrus properties measured by lidar in the NH have been developed, allowing an interpretation of our results in a broader context [*Sassen and Campbell*, 2001; *Goldfarb et al.*, 2001].

2. Experimental Methods

2.1. Instrumentation

[5] The data presented here were measured with the MARL (*M*obile *A*erosol *R*aman *L*idar) - system, a backscatter lidar based on a linear polarized Nd:YAG Laser with 30 Hz repetition rate and 200 mJ pulse energy at 532 nm and 355 nm. The lidar is mounted in a standard 20 ft container and therefore is mobile in a sense that it can be shipped to any desired place, with the only operation requirement being a 10 kW power supply at the site [*Schäfer et al.*, 1995]. The system, originally designed for stratospheric aerosol measurements, was adjusted to perform measurements of tropospheric aerosols and clouds in 1999. The 9-channel detector measures elastic backscatter at 355 and 532 nm separated for polarization. Additional N_2-Raman channels at 387 and 607 nm provide the opportunity to perform extinction measurements. The system is generally operated with a time resolution of 140 s and a range resolution of 7.5 m. A small field of view and narrowband optical filters allow daytime operation. During the campaigns the system was measuring continuously, with precipitating or dense cloud cover as the only limiting factor.

2.2. Data Analysis

[6] To detect clouds in the upper troposphere, the backscattered light is analyzed in respect to peaks that result from enhanced backscattering from cloud particles. Every significant peak in the lidar signal indicates the presence of a cloud. Detecting the perpendicular polarization makes this method very sensitive in the case of non-spherical cloud particles. The lower detection limit of MARL

0094-8276/02/2002GL015077$05.00

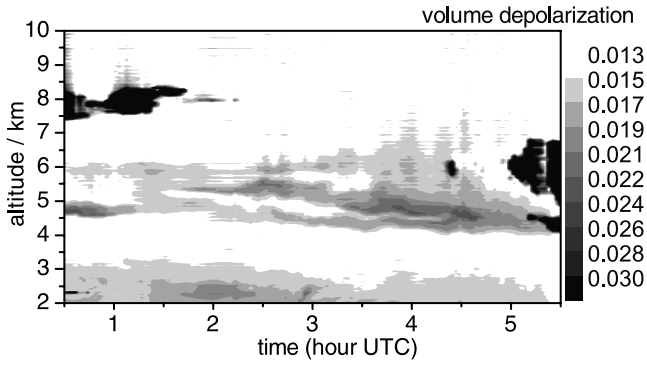

Figure 1. Lidar measurements (depolarization versus altitude) of clouds and aerosols on October 9 2000. Very thin layers of "haze clouds" ($\tau < 10^{-3}$) in the altitude from 4 to 6 km are followed by ice cloud formation. According to trajectory runs the air mass holding the aerosol is of arctic origin.

roughly corresponds to clouds with a backscatter ratio $R_L = 2$ and a thickness of about 30 m. The optical depth (τ) of such a cloud can be estimated to be well below 10^{-3}. The upper detection limit is reached when no detectable signal arrives at the cloud top, which is the case for $\tau \geq 3$. Thus, the range of detection extends from tenuous haze layers up to mature cirrus clouds. Among all detected clouds, cirrus is identified by a particle depolarization at 532 nm (δ) larger than 0.1, indicating that the cloud consists of frozen particles.

[7] The lidar signals are inverted using a modified Klett algorithm [*Klett*, 1985]. The clouds' optical depth can be determined using a method suggested by *Ansmann et al.* [1992] based on the Raman signals. During daytime this method is not applicable due to a bad signal to noise ratio. In this case τ can still be evaluated by assuming a homogeneous aerosol-load in the upper troposphere. The optical depth can then be calculated by considering the signal decay from above compared to that below the cloud: Defining $R'(r)$ as the ratio of the measured lidar return P(r) to a pure molecular model curve $P_{Ray}(r)$:

$$R' = P(r)/P_{Ray}(r);$$
$$P_{Ray}(r) = C/R^2 \beta_{Ray}(r) \exp\left[-2 \int_0^r \alpha_{Ray}(r')dr'\right] \quad (1)$$

α_{Ray} extinction coefficient by molecules
β_{Ray} backscatter coefficient by molecules
C calibration constant

The optical depth can be expressed as $\tau = \ln (R'_{uc}/R'_{lc})$, with R'_{uc} and R'_{lc} being the R' above and below the cloud respectively. We will refer to this method as the "R-method". It is limited due to an estimated uncertainty in the aerosol load to $\tau > 0.1$ at 532 nm and $\tau > 0.05$ for 355 nm. Assuming a constant extinction to backscatter ratio (α/β, "lidar ratio") within a cloud, the extinction and backscatter profiles can be calculated from the inverted signals and τ. There is a good correlation between the R- and the Raman-method in those cases where both are applicable. This indicates that generally the extinction profile measurements performed by the MARL system are of high quality.

[8] Where both methods fail, τ is determined by the pure Klett-method assuming a lidar ratio of 25 sr. The particle depolarization profile $\delta(r)$ is retrieved using the standard procedure described by *Beyerle et al.* [2001].

3. Observations

[9] In PA we find cirrus during 56% of the measured time, i.e., more frequently than in PW, where ice clouds occurred only in 35% of the measurements. This difference is most likely due to different weather conditions. The meteorological situation in PA was characterized during most of the campaign period by a zonal jet stream further south, sending a series of frontal systems to the PA area. Cirrus was observed mostly within the lifted warm air preceeding the front. In Prestwick, the meteorological situation was more complex and therefore more difficult to interpret. For quite a long period it was characterized by a stationary planetary wave with a low centered northwest of Ireland. The rather stable conditions were only sometimes interrupted by minor disturbances and account for the lower occurrence frequency of cirrus in PW.

[10] Thus, it is very surprising that the mean macrophysical properties of the clouds given in Table1 agree very well between PA and PW. These values are compared with climatologies established by long-term lidar measurements at the Observatoire Haute Provence, France (OHP, [*Goldfarb et al.*, 2001]) and in Salt Lake City, USA (SLC, [*Sassen and Campbell*, 2001]). We find that most of the differences may be explained by the elevation of the tropopause towards lower latitudes. As a consequence, cirrus top heights as well as the mean thickness are increasing with decreasing latitude. The cloud base temperatures on the other hand coincide well among our campaigns and with *Sassen's* climatology. Even though this temperature of 234 K corresponds to the threshold where homogenous freezing occurs [*Hobbs*, 1993], it is a mean value and should not be mixed up with an existence temperature for ice clouds. In fact we find cirrus clouds with $\delta > 0.1$, up to a temperature of 260 K equally often at both locations.

[11] During the PW campaign thin layers of particles have been observed on six occasions in an altitude between 5 and 8 km with optical depths estimated to be below 10^{-3} (Figure 1). According to the above "lidar-based" definition, these layers have to be considered as a cloud. They do differ from other subvisible clouds by their very low and fairly stable optical depth. In some cases they are in connection with the formation of thicker clouds. Trajectory calculations do not yield a clear picture of the aerosol's origin. Since these layers show only little depolarization, they are not considered as cirrus (and therefore are not included in the statistics of Table 1). There are no corresponding observations from PA.

[12] It should be mentioned that in PW on September 25/26, 2000, we detected for about 3 hours a non-depolarizing and very steady cloud layer in an altitude of 15 km, about 3 km above the tropopause.

4. Discussion

[13] Given the different meteorological conditions during the campaigns, it is amazing that optical depth mean values of 0.25 and 0.26 are nearly the same in Punta Arenas and in Prestwick, respectively. This consistency still applies when

Table 1. Mean Values for the Cloud Properties From the INCA Campaigns (Median value in brackets)

	Punta Arenas	Prestwick	OHP (fall) [*Goldfarb et al.*, 2001]	SLC (Oct–Dec means) [*Sassen and Campbell*, 2001]
Location	53.1°S, 71°W	55.5°N, 4.6°W	44°N, 6°E	41°N, 112°W
Measured period	71 hours within 3 weeks	74 hours within 3 weeks	∼2300 h within 6 years	∼2200 h within 10 years
Cirrus occurrence frequencies (%)	56	35	57	–
Cloud base height (km)	8.0 (7.9)	8.3 (8.5)	9.3	8.9
Cloud top height (km)	9.5 (9.8)	9.6 (10.1)	10.7	11.1
Cloud thickness (km)	1.4 (1.1)	1.2 (0.8)	1.4	1.9
Distance to tropopause (km)	1.7 (1.7)	1.0 (0.8)	0.8 (∼0.2)	0.4
Cloud base temperature (K)	234 ± 12	234 ± 13	–	234
Cloud top temperature (K)	224 ± 10	225 ± 12	–	217
Cloud mean temperature (K)	229 ± 9.5	230 ± 11	–	–
Optical depth @532 nm	0.27 (0.08)	0.28 (0.11)	.07	0.42
Extinction (km-1) @ 532 nm	.19 (0.06)	.20 (0.12)	–	–
Lidar ratio (sr-1) (@532 nm)	26	23	18.2 (assumption)	
Lidar ratio (sr-1) (@355 nm)	25	22		

looking at the frequency of occurrence distribution (FOD) of the optical depth. Figure 2 shows the FOD for the PW and PA datasets plotted as d $p(\tau)$/d logτ, with $p(\tau)$ normalized to 1. This plot can be interpreted as the likelihood of encountering a cloud with an optical depth in the order of magnitude of τ (i.e., d logτ = 1) among all detectable cirrus clouds. Both distributions show a very similar shape with a maximum at about $\tau = 0.3$ on the logarithmic scale. The decrease on the right side is due to the instruments' cut off at about $\tau \approx 3$. However, there is no conceivable reason why the lidars' response should not be linear in the range between 10^{-3} and 0.5. It is therefore very unlikely that the instrumental technique causes the remarkable agreement between the two curves.

[14] In Figure 2 the results from SLC and OHP are plotted along with our data. Most of the differences between the curves can be explained by different upper detection limits of the instruments. This is also reflected in the mean optical depths given in Table 1. In the data from the OHP, thick cirrus ($\tau > 0.1$) occurs less frequently. However, this is most likely due to the measurement technique that was used. (If one increases the relative abundance of thick cirrus the OHP-curve does not look that different from the other curves.)

[15] Comparisons with climatologies from satellite observations are not easy to accomplish. The occurrence frequencies supplied by *Wang et al.* [1996] from SAGE II observations can not be translated easily to the data given here, due to the different observational technique and a completely different way to detect and define cirrus. However, they support our findings of an occurrence frequency at around 20% for subvisible clouds in the midlatitudes.

[16] The common feature that may be established from the lidar data is a slight and steady decrease of the abundance of clouds with decreasing order of magnitude of the optical depth. It reaches zero for $\tau < 10^{-3}$, a value characteristic for layers of aerosol particles rather than ice clouds. We do not find a natural threshold separating aerosol from subvisible clouds and thin from thick cirrus. We rather find a smooth transition supporting the idea, that cirrus formation goes through a haze state as expressed by *Heintzenberg et al.* [1995] and that this process is rather slow. The shape of the frequency distributions suggests, that this growth (or decay) of cirrus obeys an exponential law with a constant coefficient throughout the observed 3 orders of magnitude of τ.

[17] The optical depth is a function of three basic values: The cloud vertical thickness D, the number density N of particles and the mean particle size, which can be expressed as equivalent particle diameter d. We do not find a linear relation between τ and D as it was reported by *Reichardt* [1999]. We rather find an exponential relationship, with the optical depth rising roughly one order of magnitude with the thickness increasing by about 600 m. Therefore the optical depth has to be a function of the particle number and/or size.

[18] So far we have discussed features that were common in both campaigns, i.e., general features of cirrus clouds. In fact, differences are hard to establish, and – given the limited measurement period – are rarely significant. Besides the haze layers mentioned in the previous chapter, there is one result that points toward an important difference in interhemispheric cirrus properties. Figure 3 shows a histogram of the frequencies of occurrence of the particle depolarization δ. In general, δ is on the order of 0.25. In PA however, we found in 18 of the 71 hours of our measurements clouds with a significantly higher δ. This type of cloud is rarely seen in PW. The depolarization is a function of the ice-crystals' shape and size. A significant change in δ

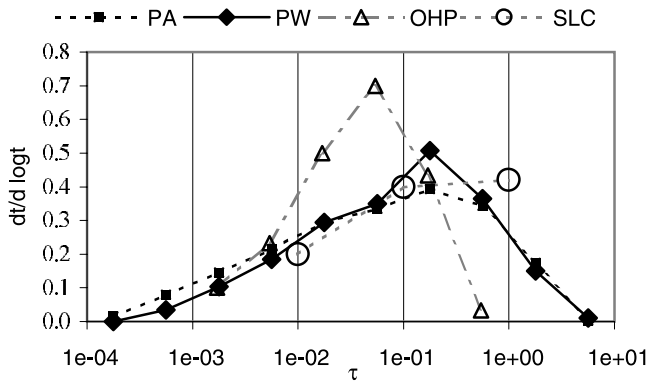

Figure 2. Frequency of occurrence of the optical depth of cirrus clouds from PA (*squares*) and PW (*diamonds*), plotted as normalized functions dt/dlogτ. The dots mark the climatology from Salt Lake City [*Sassen and Campbell*, 2001] for thick ($\tau > 0.3$), thin ($0.03 < \tau < 0.3$) and subvisible ($\tau < 0.03$) cirrus. The triangles mark the results measured at the Observatoire Haute Provence (OHP) reported by *Goldfarb et al.* [2001].

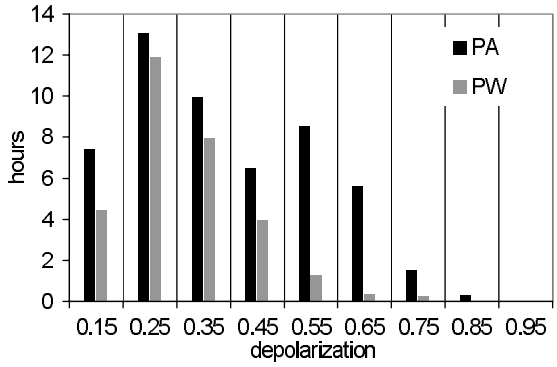

Figure 3. Histogram of depolarization measurements in 0.1 wide bins. Most ice clouds show a depolarization around 0.25. In PA, a huge number of clouds show high depolarization above 0.45.

indicates a different crystal habit, which in turn is the result of the formation mechanism. In PA and PW about 95% of the highly depolarizing clouds have a top temperature below 235 K, meeting the requirement for homogenous freezing. In contrast, 25% of the ''normally depolarizing type'' are warmer than the threshold temperature for homogeneous freezing, suggesting that the ice has formed by heterogeneous nucleation. Non-spherical scattering computations indicate that high depolarization ratios are caused by nearly spherical shapes rather than non-spherical geometries e.g., cylinders [*Liu and Mishchenko*, 2001]. It is therefore possible that the 'high δ'-type consists of frozen droplets, rather than crystals that have grown in the solid state. This is also supported by the finding that in PA liquid water clouds were found up to the temperature level of 238 K (67%-quantil), while in PW they are only found up to 252 K.

5. Conclusions

[19] The most interesting difference between the southern and the northern datasets is found in the depolarization behavior of cirrus clouds. We may distinguish two types of clouds, one showing a much higher depolarization ($\delta > 0.45$) than the other ($\delta \approx 0.25$). From an analysis of the cloud top temperatures and scattering theory we conclude that homogeneous freezing is the predominant formation mechanism for the high-δ-type. This is supported by the fact that the aerosol load in the NH is higher than in the south, a well known fact which is also reflected in our lidar data in the form of very thin haze layers. These aerosol particles may supply a sufficient number of freezing nuclei in the NH, where as a result we find only 6% of all cirrus highly depolarizing versus 30% in PA (SH).

[20] We do not find a significant difference in 'macrophysical' properties like mean altitudes or optical depth of cirrus between northern and the southern hemisphere. The ability of our lidar system to measure clouds with optical depths covering nearly 4 orders of magnitude reveal in both cases a frequency of occurrence of τ that continuously increases approximately linear with log(τ) in accordance with climatological lidar and satellite data. The onset for cirrus formation must therefore be identified as the point where the curves in Figure 2 reach zero. This point is near or below the lower detection limit of state-of-the-art lidar systems. In terms of the extinction coefficient this limit is around $\alpha \approx 10^{-3}$ km^{-1} (at 532 nm), a value which is on the order of magnitude of tropospheric background aerosol. We realize that lidar observations are not a Lagrangian experiment. However, our results suggest that cirrus formation is a continuous process with a constant growth coefficient starting right from the aerosol stadium.

[21] Since the dataset presented here is very limited in time and space more and long-term measurements are required from different parts of the world to back up our findings. As the only instruments capable of detecting cirrus clouds from the ultra-thin to visible range lidars provide very useful information and should play an important role in future research and long-term observational sites focusing on cloud studies.

[22] **Acknowledgments.** We would like to thank I. Beninga and W. Ruhe (Impres GmbH.) as well as T. Ronge for their support. We also thank all members of the INCA crew for the great collaboration in the field and BADC for the calculation of trajectories and access to data of the European Center for Medium-range Weather Forecast (ECMWF).

References

Ansmann, A., U. Wandinger, M. Riesbell, C. Weitkamp, and W. Michaelis, Independent measurement of extinction and backscatter profiles in cirrus clouds by using a combined Raman elastic-backscatter lidar, *Appl. Opt.*, *31*, 7113–7131, 1992.

Beyerle, G., M. R. Gross, D. A. Haner, N. T. Kjome, I. S. McDermid, T. J. McGee, J. M. Rosen, H.-J. Schäfer, and O. Schrems, A Lidar and Backscatter Sonde Measurement Campaign at Table Mountain during February–March 1997: Observations and cirrus clouds, *J. Atmos. Sci*, *58*, 1275–1287, 2001.

Goldfarb, L., P. Keckhut, M.-L. Chanin, and A. Hauchecorne, Cirrus Climatological Results from Lidar Measurements at OHP (44°N, 6°E), *Geophys. Res. Lett.*, *28*, 1687–1690, 2001.

Heintzenberg, J., Y. Fouquart, A. Heymsfield, J. Ström and G. Brogniez, Interactions of Radiation and Microphysics in Cirrus, Clouds, in Chemistry and Climate, edited by P. J. Crutzen and V. Ramanathan, pp. 29–55, Springer Verlag, Berlin, 1995.

Hobbs, P. V., Aerosol-cloud interactions, in Aerosol-Cloud-Climate Interactions, edited by P. V. Hobbs, pp. 33–73, Academic Press, San Diego, 1993.

Klett, J. D., Lidar inversion with variable backscatter/extinction ratios, *Appl. Opt.*, *24*, 1638–1643, 1985.

Liu, L., and M. I. Mishchenko, Constraints on PSC particle microphysics derived from lidar observations, *J. of Quant. Spec. Radiat. Trans.*, *70*, 817–831, 2001.

Liou, K.-N., The influence of cirrus on weather and climate processes: A global perspective, *Mon. Wea. Rev.*, *114*, 1167–1199, 1986.

Reichardt, J., ''Optical and geometrical properties of northern midlatitude cirrus clouds observed with a UV Raman lidar'', *Phys. Chem. Earth (B)*, *24*(3), 255–260, 1999.

Sassen, K., and J. R. Campbell, A midlatitude cirrus cloud climatology from the facility for atmospheric remote sensing. Part I: Macrophysical and synoptic properties, *J. Atmos. Sci.*, *58*, 481–496, 2001.

Sassen, K., M. K. Griffin, and G. Dodd, Optical Scattering and microphysical Properties of Subvisual Cirrus Clouds and Climatic Implications, *J. Appl. Meteor.*, *28*, 91–98, 1989.

Schäfer, H.-J., O. Schrems, G. Beyerle, B. Hofer, W. Mildner, F. A. Theopold, W. Lahmann, C. Weitkamp, and M. Steinbach, A modular and multi-purpose lidar system for observation of tropospheric and stratospheric aerosols, *SPIE EurOpto Ser.*, *2581*, 128–136, 1995.

Tegen, I., P. Hollrig, M. Chin, I. Fung, D. Jacob, and J. Penner, Contribution of different aerosol species to the global aerosol extinction optical thickness: Estimates from model results, *J. Geophys. Res.*, 23,895, 1997.

Wang, P.-H., P. Minnis, M. P. McCormick, G. S. Kent, and K. M. Skeens, A 6-year climatology of cloud occurrence frequency from Stratospheric Aerosol and Gas Experiment II observations (1985–1990), *J. Geophys. Res.*, *101*, 29,407–29,429, 1996.

Zhang, Y., A. Macke, and F. Albers, Effects of crystal size spectrum and crystal shape on stratiform cirrus radiative forcing, *Atmos. Res.*, *52*, 59–75, 1999.

F. Immler and O. Schrems, Alfred Wegener Institute for Polar and Marine Research, Bremerhaven, Germany.